



Enhancement of Optical Spin-Orbit Coupling in Anisotropic ENZ Metamaterials

Vittorio Aita , *Student Member, IEEE*, and Anatoly V. Zayats 

Abstract—Vector vortex beams which possess complex intensity and polarisation patterns, and phase or polarisation singularities are important in a variety of applications ranging from high resolution imaging and data transmission to nonlinear optics and quantum technologies. Here, we theoretically analyse the effect of vector vortex beams propagation through strongly anisotropic metamaterials exhibiting epsilon-near-zero behaviour. The interaction of the metamaterial with longitudinal field of the vector beams results in a strong modification of the polarisation distribution, with the metamaterial acting as an azimuthal polariser. The dependence on the local ellipticity of the field is also investigated revealing conversion of spin angular momentum to orbital angular momentum and polarisation structure vorticity, mediated by the longitudinal field. The results show the promise of an anisotropic metamaterial platform for manipulation of polarisation properties of and spin-orbit coupling in vector vortex beams.

Index Terms—Epsilon-near-zero, hyperbolic metamaterials, spin-orbit coupling, vector vortex beams.

I. INTRODUCTION

VECTOR vortex beams (VVBs) with complex polarisation patterns and orbital angular momentum (OAM) are important for designing unusual light-matter interactions and addressing quantum and optical properties of matter, such as forbidden optical transitions in atoms and quantum dots, optical trapping and manipulation, information encoding, superresolution microscopy and many others [1]. VVBs are instrumental for realisation of topologically protected polarisation textures of light, such as skyrmions, merons and hopfions [2], [3], [4]. VVBs can be commonly seen as the superposition of two orthogonally polarised scalar optical vortices, each possessing a phase singularity in the centre of the beam [5]. Such superposition can in turn lead to the generation of a polarisation singularity [6], as is the case of the two archetypal types of vector beams: radially and azimuthally polarised beams, which carry a polarisation singularity collocated with strong longitudinal electric or magnetic field, respectively, in the centre of the beam [7]. Due to the intimate link between transverse and longitudinal fields required by the Maxwell's equations,

this results in the possibility to generate a longitudinal field whose characteristics can be defined by the transverse state of polarisation (SOP), even in the case of a paraxial beam [8], [9], [10], [11], [12]. Moreover, the longitudinal field depends on the OAM carried by the beam due to spin-orbital angular momentum conversion, opening up additional opportunities for the field manipulation.

Due to the complex balance of the electric field components in VVBs, strong focusing [13], [14], [15], [16] or anisotropic media [17], [18], [19] can be used to manipulate the beam polarisation properties by differently influencing the transverse and longitudinal field components. In this respect, hyperbolic metamaterials [20], [21], which exhibit record optical anisotropy since they behave as a dielectric ($\text{Re}(\epsilon) > 0$) for one polarisation of light and as a metal ($\text{Re}(\epsilon) < 0$) for the other [22], [23], [24], [25], provide unique opportunities for manipulation of VVBs and spin-orbit coupling. Moreover, due to their intrinsic properties, hyperbolic metamaterials support the so-called epsilon-near-zero (ENZ) regime, in which their interaction with transverse and longitudinal electric field components are strongly different.

In this paper, we investigate how VVBs of different orders interact with hyperbolic metamaterials formed by arrays of plasmonic nanorods. A generalised version of a radial beam was studied, which is allowed to possess topological charge (TC) higher than one. We show that in the case of VVBs with locally linear SOP, the coupling of the longitudinal field with the ENZ-related resonance of the metamaterial is able to modify the polarisation of the beam, making it almost purely azimuthal (we refer to this phenomenon as “azimuthalisation”) for every value of topological charge apart from $\ell = 1$. In the latter case of $\ell = 1$, the longitudinal field is regenerated from the transverse one due to the symmetry of the beam. However, in the case of a non-ideal radial polarisation with non-zero local ellipticity (non-zero spin), the radial polarisation loses its resilience to azimuthalisation. The metamaterial acts as an azimuthal polariser in the ENZ spectral range with the degree of azimuthalisation controlled by the metamaterial thickness and a choice of an operating wavelength. At the wavelengths away from the ENZ region, in the case of polarisation states with spin angular momentum, pronounced vorticity of the SOP after propagation through the metamaterial is observed due to spin-orbit coupling. The handedness of the resulting polarisation vortex depends on the metamaterial dispersion regime.

Manuscript received 21 November 2022; revised 21 December 2022; accepted 23 December 2022. Date of publication 27 December 2022; date of current version 12 January 2023. This work was supported by ERC iCOMM Project under Grant 789340. (*Corresponding author: Vittorio Aita.*)

The authors are with the Department of Physics and London Centre for Nanotechnology, King's College London, Strand, London WC2R 2LS, U.K. (e-mail: vittorio.aita@kcl.ac.uk; a.zayats@kcl.ac.uk).

Digital Object Identifier 10.1109/JPHOT.2022.3232460

II. THEORETICAL APPROACH

A. Vector Vortex Beams With Arbitrary Polarisation States

In the paraxial approximation, for a monochromatic beam propagating along the optical axis of a uniaxial, nonmagnetic and nongyrotropic medium, the Maxwell's equations imply a strong relation between the electric field components in the $x - y$ plane transverse to the propagation direction and its component along z :

$$\nabla \cdot \hat{\epsilon} \mathbf{E} = \epsilon_T \nabla_T \cdot \mathbf{E}_T + \epsilon_z \partial_z E_z = 0, \quad (1)$$

where $\mathbf{E}_T = (E_x, E_y)$ and E_z are the transverse and longitudinal components of the electric field, respectively, $\nabla_T = (\partial_x, \partial_y)$, and $\hat{\epsilon} = \text{diag}(\epsilon_T, \epsilon_T, \epsilon_z)$ is the permittivity tensor. For an isotropic medium, $\hat{\epsilon} = \text{diag}(\epsilon)$, and (1) reduces to $\nabla_T \cdot \mathbf{E}_T = -\partial_z E_z$. Equation (1) illustrates that any modification of either the intensity distribution of the transverse field E_T or its SOP will lead to modifications of E_z . It naturally comes from this observation that the more pronounced the variations of the electric field over the transverse plane are, the stronger longitudinal field can be generated. In this framework, structuring the polarisation of the beam allows for more degrees of freedom to control the electric field transverse gradient and hence the longitudinal component, especially if the realised SOP is non-uniform.

A general set of VVBs can be described in the basis of two orthogonal linear polarisations $\{|H\rangle, |V\rangle\}$ as [26]

$$|H, \ell\rangle = \cos \ell\phi |H\rangle + \sin \ell\phi |V\rangle \quad (2a)$$

$$|V, \ell\rangle = -\sin \ell\phi |H\rangle + \cos \ell\phi |V\rangle, \quad (2b)$$

where ϕ is the azimuthal angle and ℓ in the topological charge. In these notations, radial and azimuthal SOPs are given by $|R\rangle = |H, 1\rangle$ and $|A\rangle = |V, 1\rangle$, therefore, they have a non-uniform polarisation distribution in the transverse plane. Although it is a locally linear pattern, the orientation of the polarisation direction changes across the beam cross-section.

Given the aforementioned decomposition, radial and azimuthal VVBs can also be considered as the superposition of two circularly polarised optical vortices (OVs) with opposite helicities ($\sigma = \pm 1$) and topological charges. Due to reciprocity, the opposite is also valid: the circular polarisation can be considered as a superposition of radial and azimuthal field distributions with a spiral phase wavefront. The more general SOPs described by (2) can be seen as the analogue of radial and azimuthal SOPs when the constitutive OVs are allowed to possess higher topological charges $\pm \ell$. Equation (2) forms an orthonormal basis in which a generic SOP, which can be found on the surface of a higher order Poincaré sphere related to the chosen value of topological charge ℓ , can be written as [26]

$$|\psi, \ell\rangle = |H, \ell\rangle \langle H, \ell | \psi, \ell\rangle + |V, \ell\rangle \langle V, \ell | \psi, \ell\rangle. \quad (3)$$

In this work, the properties of optical beams with various SOPs described by (3) are analysed under different focusing conditions and upon propagation through an anisotropic metamaterial. For simplicity, each SOP will be labelled as $|\psi, P_H(\psi), P_V(\psi), \ell\rangle$, where $P_H(\psi)$ and $P_V(\psi)$ represent the projections of the state $|\psi\rangle$ onto the basis $\{|H, \ell\rangle, |V, \ell\rangle\}$

described by (2), normalised to one. In particular, given the azimuthalisation nature of the phenomenon studied below, we focus on initial SOPs described by $|\psi, P_H(\psi), 0, \ell\rangle$ which can be seen as a set of generalised radial beams with arbitrary topological charge ℓ . The analogous set of generalised azimuthal SOPs $(|\psi, 0, P_V(\psi), \ell\rangle)$ does not give rise to interesting polarisation changes with regard to its electric field. A further analysis of the magnetic field of an azimuthally polarised beam, is beyond the scope of this paper.

B. Effective Medium Theory for Metamaterials

The metamaterial considered in this study consists of a two-dimensional array of plasmonic (gold) nanorods, embedded in an alumina matrix (Fig. 1). Due to the deep subwavelength dimensions of the meta-atoms, such a metamaterial is well described by the effective medium theory (EMT), using the Maxwell-Garnet approximation. The plasmonic nanorods are considered as metallic inclusions in a dielectric matrix. Within the EMT framework, a finite thickness (h) slab of such a metamaterial can be considered as an uniaxial crystal with an optical axis oriented along the nanorods (z -direction). The permittivity tensor of this medium can be described by the diagonal matrix $\hat{\epsilon} = \text{diag}(\epsilon_x, \epsilon_y = \epsilon_x, \epsilon_z)$ with [27]

$$\epsilon_x = \epsilon_y = \epsilon_m \frac{(1 + \eta)\epsilon_m + (1 - \eta)\epsilon_d}{(1 - \eta)\epsilon_m + (1 + \eta)\epsilon_d} \quad (4a)$$

$$\epsilon_z = \eta\epsilon_m + (1 - \eta)\epsilon_d. \quad (4b)$$

Here, ϵ_m and ϵ_d are the permittivity of the metal and the dielectric matrix, respectively, and $\eta = \pi(r/p)^2$ is the filling factor of the metallic inclusions in the matrix, where r is the radius of the nanorods and p is the periodicity of the square array.

For the metamaterial considered throughout this work, the geometrical parameters are chosen to be: $h = 370$ nm, $r = 20$ nm, and $p = 80$ nm. The permittivity of the host medium (Al_2O_3) has been taken from Ref. [28], while the permittivity of gold from Ref. [29]. The effective permittivities show the typical behaviour of a hyperbolic metamaterial (Fig. 1(b)). In particular, $\text{Re}(\epsilon_z)$ is positive (negative) in a shorter (longer) wavelengths range, exhibiting a dielectric (metallic) behaviour. The zero-crossing point $\text{Re}(\epsilon_z) \approx 0$ defines the ENZ region, which is found at a wavelength $\lambda_{\text{ENZ}} \approx 655$ nm for the metamaterial studied.

The transmission of light through the metamaterial was calculated using the transfer matrix method (TMM) [30]. In order to reproduce the structure of an experimental realisation of the metamaterial, a three-layer structure was considered (Fig. 1(a)), where the first layer is semi-infinite free space ($\epsilon_1 = 1$), the second one is the metamaterial ($\epsilon_x = \epsilon_y; \epsilon_z$), and the third is semi-infinite glass ($\epsilon_3 = 2.25$). Assuming light propagates through the system from free space, the continuity of the transverse electric field at both interfaces (free-space/metamaterial and metamaterial/glass) is imposed to obtain the Fresnel coefficients. Hence, the electric fields reflected and transmitted at each interface can be obtained directly from the initial field and eventually recombined to retrieve the total field in every spatial region. The resulting extinction spectrum is related to

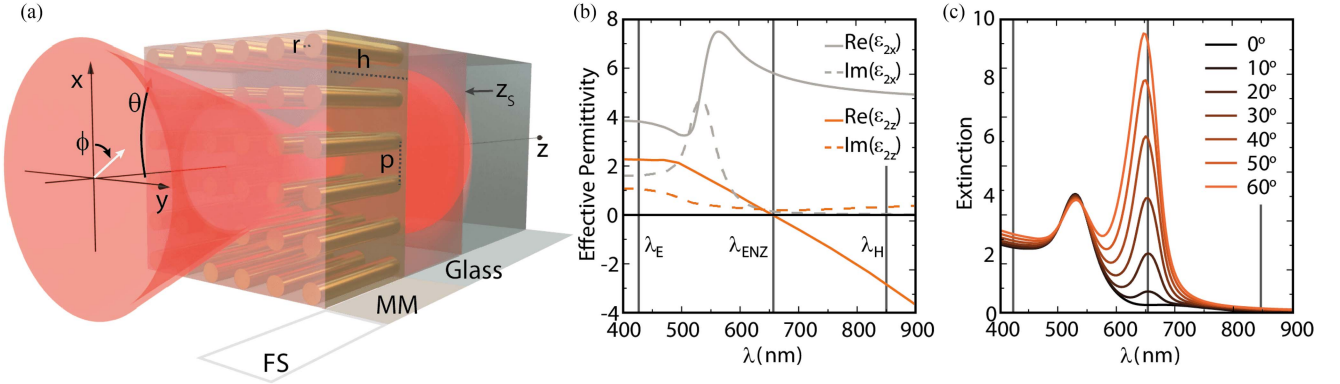


Fig. 1. (a) Geometry of the illumination: light propagates along the positive z direction and is focused in the middle of the metamaterial (MM). The x - y plane is referred to as the transverse plane. The intensity and polarisation distributions are calculated in the plane $z = z_S$. The coordinate system and the angular variables θ and ϕ are shown. Geometrical parameters of the metamaterial are also indicated. (b) Real and imaginary parts of the diagonal components of the effective permittivity tensor obtained in the EMT framework. (c) Simulated extinction spectra of the metamaterial for the TM-polarised plane wave illumination at various angles of incidence. The parameters of the metamaterial are specified in Section II B. Vertical lines indicate the wavelengths, corresponding to different dispersion regimes, at which VVBs propagation was studied: $\lambda_E = 430$ nm ($\lambda_H = 850$ nm) for the elliptical (hyperbolic) dispersion regime and $\lambda_{ENZ} = 655$ nm for the ENZ regime.

the metamaterial permittivity spectra and has two features: a short-wavelength one related to the absorption in Au, observed for all the polarisations of incident plane waves and independent of the angle of incidence, and the long-wavelength one near the ENZ condition, which is observable only for illumination with an electric field component parallel to the nanorods (Fig. 1(c)). Therefore, at normal incidence, a plane wave cannot couple to the ENZ-related resonance, the same as a weakly focused Gaussian beam which possesses a negligible longitudinal field. However, in the case of VVBs propagating along the optical axis of the metamaterial, the coupling of this resonance to the longitudinal field component can be exploited to strongly modify the polarisation distribution across the beam, even at normal incidence. In turn, the extinction of the VVB depends on its parameters (cf. Fig. 1(c) and Fig. 2(i)–(k)).

C. Simulation Framework

The propagation of the beam with the chosen SOP has been simulated using the Richards-Wolf theory for vectorial diffraction [17], [31], [32], [33], applying it to the case of VVBs propagating through a slab of an anisotropic material. The field is obtained integrating its angular spectrum over a region in the momentum space fixed by the numerical aperture (NA) of the focusing system [34]. To fully characterise the spectrum, the amplitude of the input field needs to be specified. For this study, the decomposition of radial and azimuthal beams into the Hermite-Gauss modes set has been used:

$$\begin{aligned} \mathbf{E}_{in}^R &= \text{HG}_{10}\mathbf{n}_x + \text{HG}_{01}\mathbf{n}_y \\ &= C f_w(\theta) (\cos \phi |H\rangle + \sin \phi |V\rangle), \end{aligned} \quad (5a)$$

$$\begin{aligned} \mathbf{E}_{in}^A &= -\text{HG}_{01}\mathbf{n}_x + \text{HG}_{10}\mathbf{n}_y \\ &= C f_w(\theta) (-\sin \phi |H\rangle + \cos \phi |V\rangle), \end{aligned} \quad (5b)$$

where $\mathbf{E}_{in}^{R,A}$ are the initial fields in the case of purely radial or purely azimuthal SOP, $\mathbf{n}_{x,y}$ are the unit vectors of the coordinate

system, the Hermite-Gauss modes are given in the polar coordinates as $\text{HG}_{10} = \cos \theta \cos \phi$ and $\text{HG}_{01} = \cos \theta \sin \phi$, C is a constant, and $f_w(\theta) = \cos \theta \exp(-1/f_0^2)(\sin^2 \theta / \sin^2 \theta_{\max})$ is the apodisation function of the system that, for simplicity of notation, also includes the θ -dependent terms contained in the modes. As can be seen from its definition, the apodisation function depends on the lens filling factor (f_0), that represents the ratio between the beam and the lens transverse size at the lens plane, and on θ_{\max} , which is the angular aperture of the lens, in turn dependent on the chosen value of NA ($\text{NA} \propto \sin \theta_{\max}$).

Comparing (5) with (2), the general expression of the incident field can be written similarly to (3) as

$$|E_{in}, E_{0x}, E_{0y}, \ell\rangle = C f_w(\theta) (E_{0x} |H, \ell\rangle + E_{0y} |V, \ell\rangle). \quad (6)$$

Given the symmetry of the system, the integration of the angular spectrum is then performed in cylindrical coordinates, taking advantage of the integral definition of the Bessel functions of the first kind. When calculations are performed for the metamaterial system, the same prescriptions are followed with a piecewise definition of the electric field. In this case, similarly to the TMM approach, the Fresnel coefficients are calculated and then included in the piecewise integration. The incident beam is focused in the middle of the metamaterial slab ($z = z_F$) where the lens focus is. All the field intensity distributions are calculated over a plane located at a geometrical distance from the focus $z_S - z_F = 10\lambda_{ENZ}$. The optical path takes into account the beam propagation through the different layers, depending on whether the simulations are carried out for propagation in free space or through the metamaterial.

III. RESULTS AND DISCUSSION

A. Azimuthalisation of VVBs With Varying Topological Charge

In order to understand the VVB propagation in a strongly anisotropic metamaterial, the SOPs of several vector field structures $|E_{in}, 1, 0, \ell\rangle$ carrying various topological charges

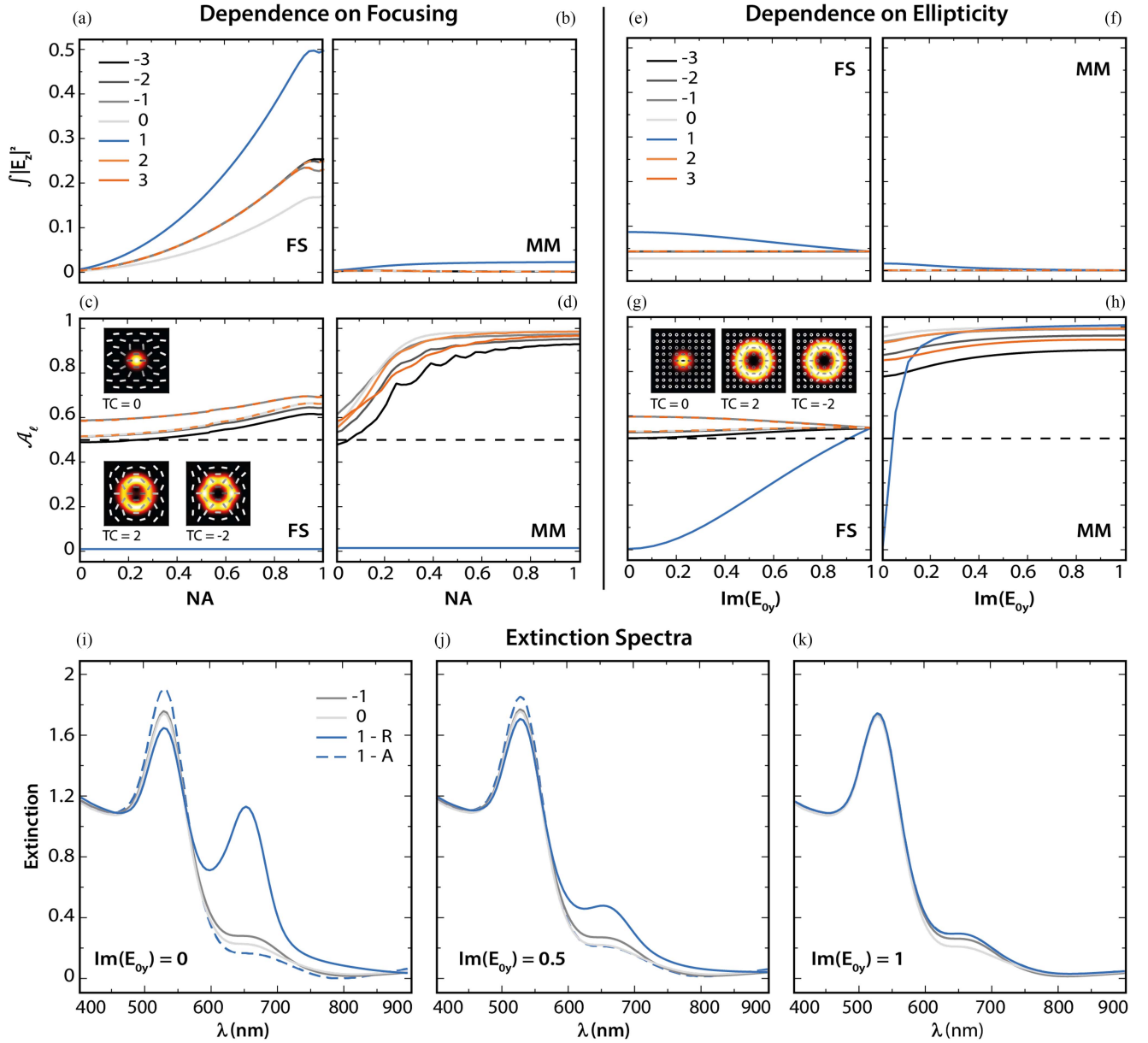


Fig. 2. (a–d) The dependence on focusing condition, described by NA, of (a,b) the longitudinal field intensity and (c,d) the azimuthal component of the SOP (7), both integrated over the transverse $x - y$ plane, for the VVBs with different topological charges ℓ propagating through (a,c) free space (FS) and (b,d) the metamaterial (MM). The incident beam is radially polarised ($E_{0x} = 1, E_{0y} = 0, |\ell| \in [0, 3]$). (e–h) The dependence on the ellipticity, described by $\text{Im}(E_{0y})$, of the same parameters as in (a–d), when the VVB is focused with $\text{NA} = 0.4$. Insets show the intensity distributions of the transverse field in the focal plane for selected VVBs together with their polarisation patterns. The wavelength corresponds to the ENZ regime $\lambda_{\text{ENZ}} = 655$ nm. The longitudinal field is normalised to the total intensity of the field. The behaviour of the integrated longitudinal intensity in (b,f) can only be distinguished between the cases $\ell = 1$ and $\ell \neq 1$ due to the overlap of all the curves for $\ell \neq 1$. In all the panels, curves are rendered with a dashed line in case of overlapping. (i–k) Extinction spectra of the metamaterial, obtained at normal incidence under tight focusing ($\text{NA} = 0.85$) of VVBs with (i) $E_{0x} = 1, E_{0y} = 0$, (j) $E_{0x} = 1, E_{0y} = 0.5i$, and (k) $E_{0x} = 1, E_{0y} = i$ for $|\ell| \in [0, 1]$. The azimuthal polarisation ($E_{0x} = 0, E_{0y} = 1, \ell = 1$, labelled as 1-A, to distinguish from the radial case 1-R) is shown for reference.

($\ell = 0, \pm 1, \pm 2, \pm 3$) were simulated under different focusing conditions after the propagation through the metamaterial at the wavelengths corresponding to different dispersion regimes and compared to free-space propagation (Figs. 2 and 3). The integral (across the beam) of the intensity distributions of the longitudinal field obtained for several VVBs indeed shows that the pure radial SOP ($\ell = 1$) exhibit the strongest longitudinal field when propagating in free space, which increases with the focusing (Fig. 2(a)).

The pronounced diffraction effects are also observed for strong focusing (Fig. 3). (The SOP of the incident VVBs (not shown in the figures) is practically indistinguishable from the free space propagation for low NAs.) After propagation through the metamaterial, the longitudinal field at the ENZ wavelength significantly decreases (Fig. 2(b)), becoming almost negligible for topological charges $\ell \neq 1$. This is due to strong extinction of the field directed along the optical axis of the metamaterial, i.e., along the nanorods (Fig. 1(c)).

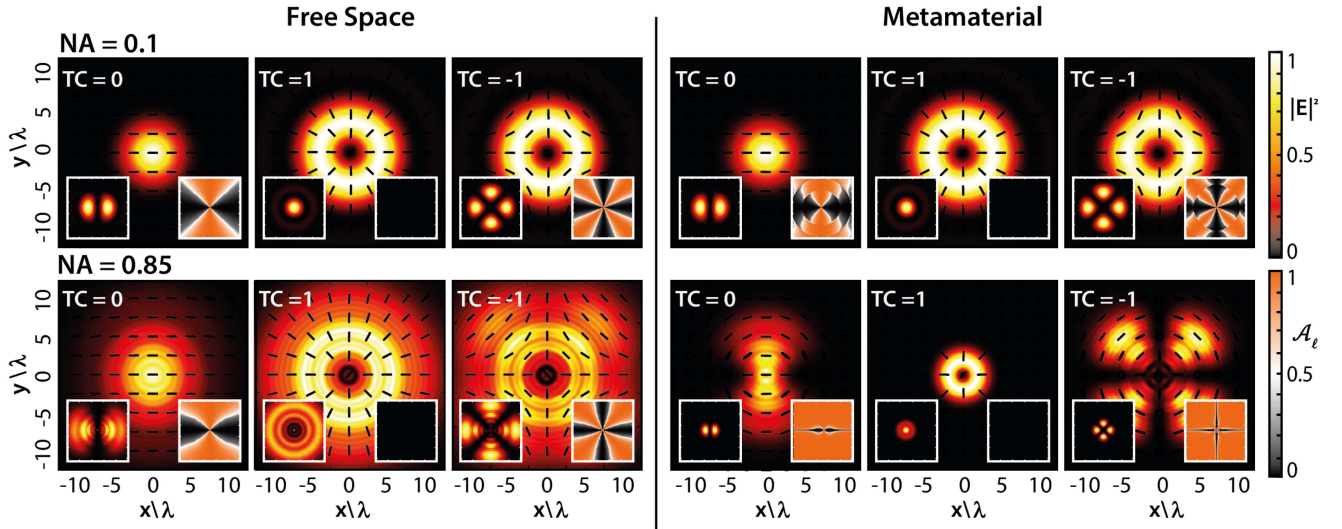


Fig. 3. Simulated intensity distributions of the transverse electric field upon propagation in free space and through the metamaterial for illumination with (top row) $NA = 0.1$ and (bottom row) $NA = 0.85$. Polarisation distributions are superimposed onto each panel. In each panel, left insets show the intensity distributions of the longitudinal field, and right insets show the projection onto the azimuthal state \mathcal{A}_ℓ (7). All intensity distributions are independently normalised to their own maximum. The SOPs of the incident VVBs (not shown) are practically indistinguishable from the free space propagation for low NA.

The effect of the metamaterial on the VVB polarisation is easy to understand comparing the intensity distributions and polarisation configurations for different focusing conditions ($NA = 0.1$ and 0.85) of the beams $|E_{in}, 1, 0, \ell\rangle$ with $\ell = 0, \pm 1$ (Fig. 3). At the ENZ wavelengths, the extinction of longitudinal and transverse fields are significantly different in the metamaterial: a strong extinction of the field along the nanorods and a weak one for the field normal to them (Fig. 1(c)). In paraxial regime (low NA), the extinction of a weak longitudinal field in the metamaterial is not significant to achieve strong modification of the transverse polarisation distribution through (1). However, for higher NA, the longitudinal field contribution to the VVB becomes important and its decrease in the metamaterial results in the azimuthalisation of the transmitted VVB for all topological charges, but $\ell = 1$ (Fig. 3). This is clearly reflected in the extinction spectra of the different VVBs (cf. Figs. 1(c) and 2(i)). While a plane wave at normal incidence is not affected by the ENZ, the ENZ-related extinction peak, observed for a plane wave illumination at oblique incidence, is indeed recovered at normal incidence for the radially polarised VVBs with a strong longitudinal field. On the other hand, when the SOP is azimuthalised and cannot support a longitudinal field, the ENZ-related extinction is suppressed.

To quantify the azimuthalisation effect, we calculate the SOP projection onto the azimuthal state $|A\rangle$ defined as

$$\mathcal{A}_\ell(x, y) = ||\langle A|E_{in}, E_{0x}, E_{0y}, \ell\rangle||^2 \in [0, 1]. \quad (7)$$

Here, the bra-ket notation is used to indicate the scalar product between the SOP of interest and the azimuthal state $|A\rangle$ and $||\cdot||$ is the norm of the scalar product. Finally, we define the ‘‘degree of azimuthalisation’’ as the integral of \mathcal{A}_ℓ over the transverse plane.

One can see a clear correspondence between the patterns where \mathcal{A}_ℓ tends to 1 (orange) and the longitudinal field intensity

tends to zero (black) (Fig. 3). Given the characteristics of the states $|R\rangle$ and $|A\rangle$, the region of lower intensity of the longitudinal field corresponds in fact to the region of stronger azimuthal component. The map of the azimuthalisation parameter $\mathcal{A}_\ell(x, y)$ shows that the azimuthalisation varies across the beam with a pattern dependent on the topological charge. The slight increase in \mathcal{A}_ℓ with NA, observed in the case of free space propagation, can be ascribed to the astigmatism the beam develops as a consequence of the tight focusing. Even for a beam as simple as a linearly polarised Gaussian beam, the transverse intensity distribution in the focal plane becomes asymmetric, resulting in small modifications of the SOP (top-left inset, Fig. 2(c)) that in turn have a non-zero contribution to the degree of azimuthalisation. Lastly, one can notice the dependence of \mathcal{A}_ℓ on the topological charge of the beam, which is inherently related to the symmetry of each SOP. The polarisation patterns of VVBs with topological charge $\ell > 0$ possess in fact an azimuthal component inherently higher than the ones of VVBs with $\ell < 0$ (cf. insets in Fig. 2(c)) due to the phase difference introduced by the topological charge.

The comparison of the SOPs of different vortex beams propagating in free space and through the metamaterial clearly shows an increase in the degree of azimuthalisation in the case of the ENZ regime and for stronger focusing, for which the longitudinal component of the field increases (Fig. 2(c),(d)). Due to the strong anisotropy and efficient interaction with the longitudinal fields, the metamaterial removes energy from the longitudinal field, breaking the balance between the transverse and longitudinal field components. How strongly the longitudinal field is reduced depends on the choice of the wavelength and/or the thickness of the metamaterial. Hence, the achieved modification of the longitudinal field weakens (or even to high degree eliminates) the radial component of the VVB beams, so that the azimuthal component of the beams becomes dominant after propagation through the metamaterial. Since azimuthal

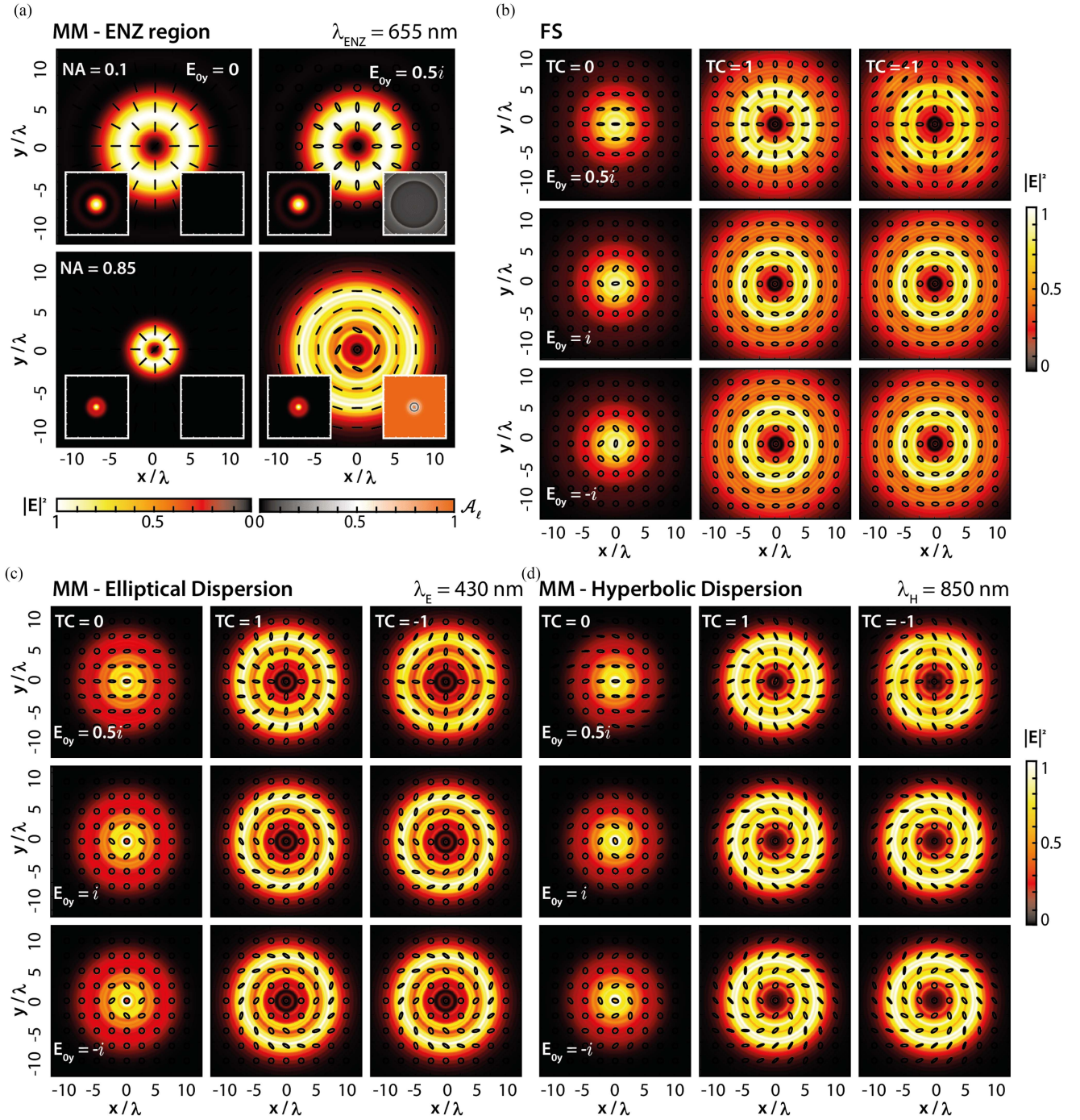


Fig. 4. Simulated intensity distributions of the transverse field components of VVBs with different ellipticity ($E_{0x} = 1$, $E_{0y} = 0.5i, i, -i$) and topological charge ($\ell = 0, \pm 1$) as indicated in the panels, for propagation (b) in free space (FS), the same for all wavelengths, and (a,c,d) through the metamaterial (MM) for the wavelengths in (a) ENZ ($\lambda_{\text{ENZ}} = 655$ nm), (c) elliptical ($\lambda_{\text{E}} = 430$ nm), and (d) hyperbolic ($\lambda_{\text{H}} = 850$ nm) regimes. Polarisation distributions are superposed on each intensity distribution. The intensity distributions are independently normalised to their own maximum. NA = 0.85 in all panels but the first row of (a) where NA = 0.1. In each panel of (a), left insets show the intensity distributions of the longitudinal field, and right insets show the projection onto the azimuthal state \mathcal{A}_{ℓ} (7).

polarisation can be represented as two opposite circular polarisations with a phase shift between them, the observed effect can be considered as a particular case of spin-orbit coupling.

These observations are consistent with the considerations that when the metamaterial removes energy from the longitudinal field, its transverse counterpart will have to re-arrange in such a

fashion that can withstand a null longitudinal field, and this can only be an azimuthal SOP, which is divergence free. The special case is a pure radial polarisation ($|E_{\text{in}}, 1, 0, 1\rangle$). In this case, even though the propagation through the metamaterial does reduce the longitudinal field intensity to a much lower value than in free space (Fig. 2), the symmetry of the transverse SOP prevents

azimuthalisation. Hence, a purely radial polarisation is shown to be resilient to the azimuthalisation induced by the interaction with the metamaterial. For the wavelengths away from the ENZ condition, where the extinction of the longitudinal field in the metamaterial is negligible at longer wavelengths or comparable to the absorption of the transverse field at shorter wavelengths (Fig. 1(c)), the balance between the field components is preserved and no appreciable azimuthalisation is observed.

B. Locally Elliptical SOPs

Any SOP decomposed onto an orthogonal basis will always possess a non-zero projection on both the basis vectors, apart when the SOP coincides with one of the basis vectors. In this regard, the resilience of the radial SOP shown in the previous section can be seen as a fundamental property of a purely radial polarisation that could potentially be affected by imperfections of the SOP pattern. One way to achieve a beam with imperfections, so far considered to be locally linear, is to introduce the local ellipticity of the SOP (i.e. adding a non-zero spin density to the initial beam). This can be achieved by increasing the imaginary part of the coefficient E_{0y} in (6) in a range $[0, 1]i$. This has a profound effect on the azimuthalisation (Fig. 2(e)–(h)).

For free space propagation, the immediate consequence of an increasing ellipticity is a decrease of the intensity of the longitudinal field for the same NA (cf. Fig. 2(a) and (e) as well as Figs. 3 and 4(a)). The weaker longitudinal field again results in the suppression of the ENZ-related extinction, even in the case of a radial SOP (Fig. 2(i),(j)). The weaker longitudinal field translates, the same as above, in azimuthalisation for all topological charges, in this case, also including $\ell = 1$. For high NA, the resilience of the original radial polarisation is lost, resulting in a SOP almost completely reshaped into an azimuthal pattern at the ENZ wavelength, both in its local linearity and its global symmetry (Fig. 4(a)). The azimuthalisation dependence on the topological charge maybe due to different phase advances dependent on the topological charge. It is also interesting to note the increase of the beam size for the not-ideal radial beam in the strong focusing regime. This can be explained by the reduction of the longitudinal field in the VVB after the azimuthalisation, which maybe essential for filtering diffraction effects.

C. Generation of Polarisation Vortices

In the case of uniform circular polarisation ($E_{0y} = \pm i$), at around the ENZ wavelength, the behaviour is very similar to the elliptical polarisation (Fig. 4(a)), with no significant improvements in the azimuthalisation observed. However, at the wavelengths away from the ENZ-related extinction, the coupling between the longitudinal field generated upon focusing and the metamaterial is decreased and, consequently, the degree of azimuthalisation for all the SOPs is visibly lowered. Counterintuitively, the additional deviation from an azimuthal pattern is observed indicating at the emergence of a polarisation vortex (Fig. 4(b)–(d)). In the case of propagation in free space (Fig. 4(b)), the SOP does not show any appreciable variation upon focusing when the value of topological charge is changed for either locally elliptical or locally circular polarisation states.

However, in the case of propagation through the metamaterial (Fig. 4(c),(d)), the emergence of a polarisation vortex is evident for all the SOPs. In this case, for purely circularly polarised beams $E_{0y} = \pm i$, vortex generation is practically independent on the topological charge if $\ell \neq 0$, and the direction of vortex does not depend on the sign of the topological charge. However, for a given value of ℓ , the orientation of the vortex flips with the SOP helicity. At the same time, for a given helicity $\sigma = \pm 1$ of the initial SOP, the vortex orientation flips with the sign of $\text{Re}(\varepsilon_z)$, when the wavelength is crossing the ENZ regime. We define the parameter $\xi = \sigma \text{sign}[\text{Re}(\varepsilon_z)]$ so that a positive value of ξ corresponds to a left handed vortex (in the observer frame), and $\xi < 0$ corresponds to a right handed vortex. For $\sigma = -1$ (Fig. 4(c),(d), bottom row), the right-handed vortex ($\text{sign}(\xi) = -1$) is observed in the elliptic dispersion regime of the metamaterial, practically absent vorticity at the ENZ wavelengths, and the left-handed vortex ($\text{sign}(\xi) = 1$) in the hyperbolic regime, related to the different phase advances in the different dispersion regimes. In the ENZ regime, the phase advance is negligible, so the vorticity can not efficiently develop while propagating in the metamaterial. The appearance of vorticity is a manifestation of the conservation of orbital momentum [35] in the spin-orbit coupling. This coupling is strongly enhanced in the metamaterial due to the associated phase evolution in the anisotropic regime. The spin-orbit coupling and the accompanying transfer of a spin momentum to an orbital momentum of light take place also in free space under strong focusing [13], [36], as it can be seen in Fig. 4(b). The latter is responsible for the observed weak vorticity in the ENZ regime (Fig. 4(a)), which is due to the propagation in free space after the metamaterial. It should be noted a nonuniform distribution of the vorticity from the beam centre. For propagation in free-space or the metamaterial in the ENZ regime, the polarisation vortex is localised near the centre of the beam, while for hyperbolic and elliptic dispersion regimes, it covers the entire cross section of the beam.

IV. CONCLUSION

We investigated how strongly anisotropic ENZ metamaterials affect polarisation properties of focused vector vortex beams, in particular generalised radial beams with higher topological charges. The propagation of VVBs through the metamaterial was simulated with the Richards-Wolf theory in the effective medium approximation for different dispersion regimes and focusing conditions. The effect of an increasing focusing power is an increase of the longitudinal field of the beam, which can be strongly modified by the metamaterial through anisotropic extinction. As a consequence of the strong relation between the transverse and longitudinal field components in the VVBs, imposed by the Maxwell's equations, the modifications of the longitudinal field alter the transverse polarisation of the beam.

It was shown that for the generalised radially polarised beams with topological charge $\ell \neq 1$, the metamaterial behaves as an azimuthal polariser for the wavelengths in the epsilon-near-zero dispersion regime, which can be considered as a consequence of spin-orbit coupling. A pure radial beam ($\ell = 1$) is however resilient to the azimuthalisation due to the phase symmetry

considerations. The resilience is lost if the symmetry is broken, for example, in the non-ideal radial beams with a non-negligible degree of local ellipticity (spin angular momentum) of the incident beam. The increase in the spin density from linear to circular polarised VVBs also leads to the generation of optical angular momentum manifesting in the rise of vortex-like behaviour in the polarisation of the beam after propagation through the metamaterial. The direction of the vorticity depends on the handedness of the incident polarisation and is different in elliptical and hyperbolic regimes of the metamaterial dispersion.

The observed effects may be useful for manipulation of vector beams with complex polarisation structures, required in imaging, metrology, data communications, material processing, atomic and molecular spectroscopy, nonlinear optics as well as quantum technologies.

DATA AVAILABILITY

All the data supporting finding of this work are presented in the Results section and are available from the corresponding author upon reasonable request.

REFERENCES

- [1] Y. Shen et al., "Optical vortices 30 years on: OAM manipulation from topological charge to multiple singularities," *Light: Sci. Appl.*, vol. 8, no. 1, 2019, Art. no. 90.
- [2] X. Lei et al., "Photonic spin lattices: Symmetry constraints for skyrmion and meron topologies," *Phys. Rev. Lett.*, vol. 127, no. 23, 2021, Art. no. 237403.
- [3] P. Shi, L. Du, C. Li, A. V. Zayats, and X. Yuan, "Transverse spin dynamics in structured electromagnetic guided waves," *Proc. Nat. Acad. Sci.*, vol. 118, no. 6, 2021, Art. no. e2018816118.
- [4] Y. Shen, B. Yu, H. Wu, C. Li, Z. Zhu, and A. V. Zayats, "Topological transformation and free-space transport of photonic hopfions," 2022, *arXiv:2207.05074*.
- [5] C. Maurer, A. Jesacher, S. Fühapter, S. Bernet, and M. Ritsch-Marte, "Tailoring of arbitrary optical vector beams," *New J. Phys.*, vol. 9, no. 3, 2007, Art. no. 78.
- [6] I. Freund, A. Mokhun, M. Soskin, O. Angelsky, and I. Mokhun, "Stokes singularity relations," *Opt. Lett.*, vol. 27, no. 7, pp. 545–547, 2002.
- [7] Q. Zhan, "Cylindrical vector beams: From mathematical concepts to applications," *Adv. Opt. Photon.*, vol. 1, no. 1, pp. 1–57, 2009.
- [8] J. Pu and Z. Zhang, "Tight focusing of spirally polarized vortex beams," *Opt. Laser Technol.*, vol. 42, no. 1, pp. 186–191, 2010.
- [9] C. Prajapati, "Study of electric field vector, angular momentum conservation and poynting vector of nonparaxial beams," *J. Opt.*, vol. 23, no. 2, 2021, Art. no. 025604.
- [10] J. Wang et al., "Exploring the ellipticity dependency on vector helical Ince-Gaussian beams and their focusing properties," *Opt. Exp.*, vol. 30, no. 14, pp. 24497–24506, 2022.
- [11] K. A. Forbes and G. A. Jones, "Measures of helicity and chirality of optical vortex beams," *J. Opt.*, vol. 23, no. 11, 2021, Art. no. 115401.
- [12] K. A. Forbes, D. Green, and G. A. Jones, "Relevance of longitudinal fields of paraxial optical vortices," *J. Opt.*, vol. 23, no. 7, 2021, Art. no. 075401.
- [13] Y. Zhao, J. S. Edgar, G. D. Jeffries, D. McGloin, and D. T. Chiu, "Spin-to-orbital angular momentum conversion in a strongly focused optical beam," *Phys. Rev. Lett.*, vol. 99, no. 7, 2007, Art. no. 073901.
- [14] P. Meng, Z. Man, A. P. Konijnenberg, and H. P. Urbach, "Angular momentum properties of hybrid cylindrical vector vortex beams in tightly focused optical systems," *Opt. Exp.*, vol. 27, no. 24, pp. 35336–35348, 2019.
- [15] H. Li, C. Wang, M. Tang, and X. Li, "Controlled negative energy flow in the focus of a radial polarized optical beam," *Opt. Exp.*, vol. 28, no. 13, pp. 18607–18615, 2020.
- [16] P. Shi, L. Du, and X. Yuan, "Structured spin angular momentum in highly focused cylindrical vector vortex beams for optical manipulation," *Opt. Exp.*, vol. 26, no. 18, 2018, Art. no. 23449.
- [17] S. Wang, X. Xie, M. Gu, and J. Zhou, "Optical sharper focusing in an anisotropic crystal," *JOSA A*, vol. 32, no. 6, pp. 1026–1031, 2015.
- [18] N. Daloi, P. Kumar, and T. N. Dey, "Guiding and polarization shaping of vector beams in anisotropic media," *Phys. Rev. A*, vol. 105, no. 6, 2022, Art. no. 063714.
- [19] Z. Liu, H. Lee, Y. Xiong, C. Sun, and X. Zhang, "Far-field optical hyperlens magnifying sub-diffraction-limited objects," *Science*, vol. 315, no. 5819, pp. 1686–1686, 2007.
- [20] V. P. Drachev, V. A. Podolskiy, and A. V. Kildishev, "Hyperbolic metamaterials: New physics behind a classical problem," *Opt. Exp.*, vol. 21, no. 12, pp. 15048–15064, 2013.
- [21] A. Poddubny, I. Iorsh, P. Belov, and Y. Kivshar, "Hyperbolic metamaterials," *Nature Photon.*, vol. 7, no. 12, pp. 948–957, 2013.
- [22] P. Ginzburg et al., "Manipulating polarization of light with ultrathin epsilon-near-zero metamaterials," *Opt. Exp.*, vol. 21, no. 12, pp. 14907–14917, 2013.
- [23] Y. Liu, G. Bartal, and X. Zhang, "All-angle negative refraction and imaging in a bulk medium made of metallic nanowires in the visible region," *Opt. Exp.*, vol. 16, no. 20, pp. 15439–15448, 2008.
- [24] K. V. Sreekanth et al., "Extreme sensitivity biosensing platform based on hyperbolic metamaterials," *Nature Mater.*, vol. 15, no. 6, pp. 621–627, 2016.
- [25] J. Yao et al., "Optical negative refraction in bulk metamaterials of nanowires," *Science*, vol. 321, no. 5891, pp. 930–930, 2008.
- [26] G. Milione, H. I. Sztul, D. A. Nolan, and R. R. Alfano, "Higher-order Poincaré sphere, Stokes parameters, and the angular momentum of light," *Phys. Rev. Lett.*, vol. 107, no. 5, 2011, Art. no. 053601.
- [27] J. Elser, R. Wangberg, V. A. Podolskiy, and E. E. Narimanov, "Nanowire metamaterials with extreme optical anisotropy," *Appl. Phys. Lett.*, vol. 89, no. 26, 2006, Art. no. 261102.
- [28] M. J. Dodge, "Refractive index," in *Handbook of Laser Science and Technology*, vol. 4. (Optical Materials, Part 2), M. J. Weber Ed. Boca Raton, FL, USA: CRC Press, 1986.
- [29] P. B. Johnson and R.-W. Christy, "Optical constants of the noble metals," *Phys. Rev. B*, vol. 6, no. 12, pp. 4370–4379, 1972.
- [30] S. Ekgasit, C. Thammacharoen, and W. Knoll, "Surface plasmon resonance spectroscopy based on evanescent field treatment," *Anal. Chem.*, vol. 76, no. 3, pp. 561–568, 2004.
- [31] B. Richards and E. Wolf, "Electromagnetic diffraction in optical systems, II. Structure of the image field in an aplanatic system," *Proc. Roy. Soc. London. Ser. A. Math. Phys. Sci.*, vol. 253, no. 1274, pp. 358–379, 1959.
- [32] K. S. Youngworth and T. G. Brown, "Focusing of high numerical aperture cylindrical-vector beams," *Opt. Exp.*, vol. 7, no. 2, pp. 77–87, 2000.
- [33] D. P. Biss and T. G. Brown, "Cylindrical vector beam focusing through a dielectric interface," *Opt. Exp.*, vol. 9, no. 10, pp. 490–497, 2001.
- [34] L. Novotny and B. Hecht, *Principles of Nano-Optics*, vol. 34. Cambridge, U.K. Cambridge Univ. Press, 2007.
- [35] A. Ciattoni, G. Cincotti, and C. Palma, "Angular momentum dynamics of a paraxial beam in a uniaxial crystal," *Phys. Rev. E*, vol. 67, no. 3, 2003, Art. no. 036618.
- [36] L. Allen, V. Lembessis, and M. Babiker, "Spin-orbit coupling in free-space Laguerre-Gaussian light beams," *Phys. Rev. A*, vol. 53, no. 5, pp. R2937–R2939, 1996.